Transient stability control of multimachine power systems using flywheel energy injection

M.-H. Wang and H.-C. Chen

Abstract: Owing to advances in many technologies, the high-speed flywheel energy storage system (FESS), flywheel battery, has become a viable alternative to electrochemical batteries and attracted much research attention in recent years. A self-organising fuzzy neural network controller is presented for FESS to improve transient stability and increase transfer capability of power systems. The main difference from a traditional control approach lies in the model-free description of the control system and parallel computing capability. Simulation results from the Taiwan power system (Taipower) show that FESS with the proposed controller has produced significant improvement in power system performance.

1 Introduction

The Taiwan power system is medium sized and isolated. With the rapid growth of high-tech industrial development in Taiwan, there exist some special characteristics of the system that include a longitudinal transmission network, a large power deficit in the north, concentration of power sources and demand, and heavy line loading [1]. Therefore, reliable power supply has become one of the most important considerations for Taipower. To solve the problem, Taiwan Power Company (TPC) has to expand the generation capacity and 345 kV transmission lines. However, the problems of environmental protection and land acquisition make the installation of new generation plants and transmission lines very difficult. It has become a critical issue for Taipower to prevent catastrophic failures and to improve the transient stability of the power system.

Transient stability is one of the most important investigations in power systems. Power companies usually operate power systems close to their thermal and stability limits. But following sudden and large disturbances, a power system may lose stability in the first swing, if it is not equipped with proper transient control devices. In the past, much research interest has been directed towards the enhancement of the transient stability of power systems, ranging from theoretical studies to advanced control devices. Recently, many researchers have employed various flexible AC transmission systems (FACTS) devices, such as braking resistors, thyristor-controlled series compensators, thyristor-controlled phase-angle shifters, unified power flow controllers, and superconducting magnetic energy storage (SMES) [1–4]. These devices have been shown to help reduce the flows in heavily loaded lines and improve stability of power systems.

Nowadays, FESS has become the most popular energy storage system because of advances in power electronics, materials and magnetic bearings [5]. The advantages of FESS against traditional batteries and SMES are higher power density, no hazardous chemicals, ease of checking the charge, insensitivity to environmental conditions and long life [5–11]. Modern FESS have been designed for a variety of applications, their capability to store energy is approximately 1–500 MJ and the peak power ranges from kilowatts to gigawatts, with the higher powers aimed at pulsed-power applications [5]. Today, power electronic devices and control systems enable FESS to respond to system disturbances within a few electrical cycles. Therefore, FESS will continue to be most popular in power system control.

Because of the advantages of FESS, this paper proposes using an FESS with a self-organising neural fuzzy controller to enhance the transient stability of multimachine power systems. The proposed controller integrates the ideas of the fuzzy logic control and neural network structure into an intelligent control system. In this NN structure, the input and output nodes represent the input speed and acceleration states, and output control signal, respectively, and the nodes in the hidden layers function as membership functions and fuzzy control rules. Initially, we set up the controller with a set of coarse fuzzy control rules that are based on a simple engineering knowledge concerning the controlled machine. Then, the fuzzy control rules and input/output fuzzy membership functions can be optimally tuned from or adapted by the backpropagation learning algorithm according to the control credit that is evaluated by a performance index table (PIT). For the robustness considered, a multilayer neural network is used to learn the relation of operating conditions and optimal parameters of the controller. A Taipower tested data set is selected for computer simulation to demonstrate the effectiveness of the proposed methodology.

2 Power system model

Because of the high cost of practical tests, this paper only uses the mathematical time simulation to prove the proposed control scheme. The model of an FESS transient control system is a nonlinear dynamic equation in multimachine power systems. An n-machine power system model, including the effects of field flux decay, damper windings, the automatic voltage regulator rotating (AVR),

IEE Proceedings online no. 20045002

doi:10.1049/ip-gtd:20045002

Paper first received 15th April 2004and in final revised form 21st November 2004. Originally published online: 23rd June 2005

The authors are with the Institute of Information and Electrical Energy, National Chin-Yi Institute of Technology, 35, 215 Lane, Sec. 1, Chung Shan Road, Taiping, Taichung, Taiwan, Republic of China

and the exciter concerning a centre of inertia (COI) rotating reference frame is given below [4, 12]:

$$\dot{\theta}_i = \tilde{\omega}_i \tag{1}$$

$$\dot{\tilde{\omega}}_i = \frac{1}{M_i}(P_{mi} - P_{ei} - P_{fbi}) - \frac{1}{M_T}P_{COI} \tag{2}$$

$$\dot{E}'_{qi} = \frac{1}{T'_{doi}}(E_{fdi} - E'_{qi}) + \frac{I_{di}}{T'_{doi}}(X_{di} - X'_{di}) \tag{3}$$

$$\dot{E}'_{di} = -\frac{1}{T'_{qoi}}E'_{di} - \frac{1}{T'_{qoi}}(X_{qi} - X'_{qi})I_{qi} \tag{4}$$

$$\dot{V}_{ri} = \frac{K_{ai}}{T_{ai}}V_{ei} - \frac{1}{T_{ai}}V_{ri} \tag{5}$$

$$\dot{V}_{fi} = \frac{K_{fi}}{T_{fi}T_{ei}}[V_{rli} - (S_{ei} + K_{ei})E_{fdi}] - \frac{1}{T_{fi}}V_{fi} \tag{6}$$

$$\dot{E}_{fdi} = \frac{1}{T_{ei}}V_{rli} - \frac{E_{fdi}}{T_{ei}}(S_{ei} + K_{ei}) \tag{7}$$

$$\dot{E}_{fessi} = P_{fbi} \tag{8}$$

$$V_{ei} = V_{refi} - V_{ti} - V_{fi} \tag{9}$$

$$V_{rli} = \begin{cases} V_{r\,max\,i} & \text{if} \quad V_{ri} > V_{r\,max} \\ V_{ri} & \text{if} \quad V_{r\,min\,i} \le V_{ri} \le V_{e\,max\,i} \\ V_{r\,min\,i} & \text{if} \quad V_{ri} < V_{r\,min\,i} \end{cases} \tag{10}$$

$$M_T = \sum_{i=1}^{n} M_i \quad \text{for } i = 1, 2, \ldots, n \tag{11}$$

where

subscript 'i' relates to the ith generator
θ_i rotor angle of generator i with respect to the COI
$\tilde{\omega}_i$ rotor speed of generator i with respect to the COI
M inertia constant
P_m mechanical power input
P_e real power output
P_{fb} input power in flywheel battery
P_{COI} COI accelerating power
E_{fd} field applied voltage
E'_d, E'_q d- and q-axis stator EMFs
I_d, I_q d- and q-axis components of armature current
X_d, X_q d- and q-axis synchronous reactances
X'_d, X'_q d- and q-axis transient reactances
V_r regulator output voltage
V_f output voltage of regulator stabilising circuit
V_t terminal voltage of generator
K_a regulator gain
K_e exciter constant related to self-excited field
K_f regulator stabilising circuit gain
S_e exciter saturation function
T'_{do}, T'_{qo} open circuit d- and q-axis time constants
T_a regulator amplifier time constant
T_e exciter time constant
T_f regulator stabilising circuit time constant
E_{fess} energy stored in flywheel battery.

In (2), the term P_{fb} represents additive real power control of FESS for the ith generator, which is determined by the proposed controller depending on the state of the generator. Figure 1 shows the schematic structure of transient stability control using FESS that includes a flywheel, a motor–generator set and control electronics with a controller for connection to an electric power system. The energy stored in a rotating mass can be found from:

$$E_{fess} = \frac{1}{2}J\omega^2 \tag{12}$$

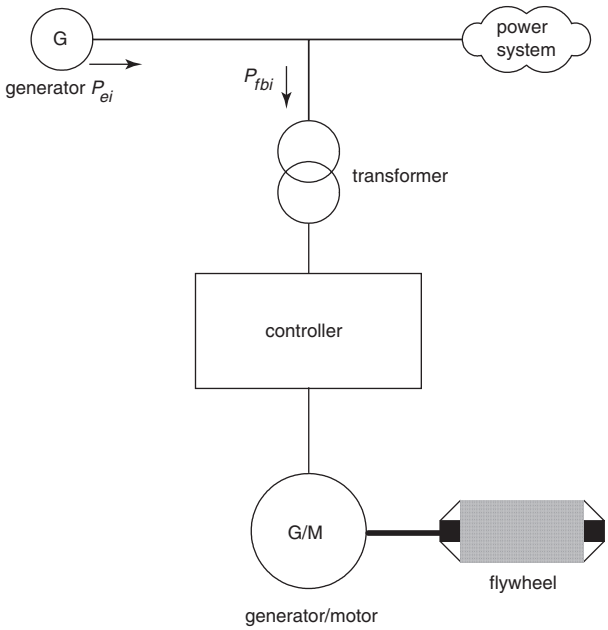

Fig. 1 *Schematic structure of FESS*

The amount of energy storage increases linearly with the moment of inertia J, and increases with the square of the rotational velocity ω. Because it is free from depth-of-discharge effects, FESS can accept and deliver large amounts of energy in a very short time [5, 9], which is a very helpful characteristic for transient stability control of power systems.

3 Proposed control system

Because of the nonlinear nature of transient stability control, a self-organising neural fuzzy controller is presented for FESS. The major difficulty in the design of a fuzzy controller arises from the determination of fuzzy control rules and input/output membership functions. Most approaches are based on expert knowledge or existing controllers, and the membership functions and/or fuzzy rules are then modified when the design fails in the test [13]. Therefore, a lot of trial-and-error effort is always required, making the design a time-consuming task. The proposed methodology is to design self-organising fuzzy systems that have capability to create the control strategy by learning. The structure of the proposed self organising fuzzy neural network controller (SONFC) is a combination of both the neural network and self-organising fuzzy control techniques. The fuzzy method provides a structural control framework to express the input/output relationship of the neural network that can embed the salient features of computation power and learning capability into the fuzzy controller.

3.1 Structure of overall control system

The overall structure of the proposed SONFC system is shown in Fig. 2. It consists of: (i) a neural fuzzy control (NFC) to control the plant, (ii) a performance index table (PIT) as an instructor for learning the control strategy, (iii) three scaling factors GS, GA, and GU to adjust the input/output values of the controller into proper ranges, which are set at 1, 0.01 and 1, (iv) a multilayer neural network (MNN) to learn the relations of operation conditions and optimal control parameters, and (v) a limiter to constrain the control action within admissible limits. Typical input variables for transient stability control are the rotor angle, angular speed, angular acceleration etc. In this work, the shaft speed and acceleration of the generator at each sample time are chosen to be input signals of the controller. The target controller output P'_{fb} is the absorbed power of FESS. The actual control signal P_{fb} can be obtained through the limiter block to satisfy practical constraints.

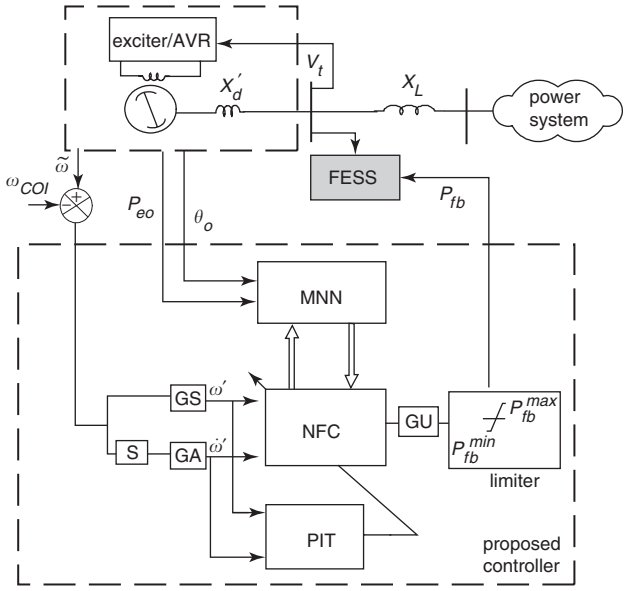

Fig. 2 *Schematic structure of proposed control system*

To implement the proposed controller, the overall operation algorithm is shown as follows:

Step 1: Set the admissible operation range of power system.

Step 2: Give a minimum operation point P_{eo}.

Step 3: Calculate the stability equipoise point of the power system.

Step 4: Set up the controller with a set of coarse fuzzy control rules, as shown in Fig. 3.

Step 5: Tune the parameters of NFC by a backpropagation learning algorithm according to the credits given in the performance index table (PIT).

Step 6: Go to step 7, if the performance index per epoch is less than a preset value, otherwise go to step 5.

Step 7: Save the optimal parameters of NFC.

Step 8: Set $P_{eo} = P_{eo} + 0.05$(p.u.).

Step 9: Go to step 10, if the P_{eo} is larger than the maximum operation point; otherwise go to step 3.

Step 10: Learn the relations of operating conditions and optimal parameters of the controller by MNN.

Step 11: Terminate the learning process, when the mean square error of the MNN is reduced to a preset value. Then, use the trained controller directly to control the power system.

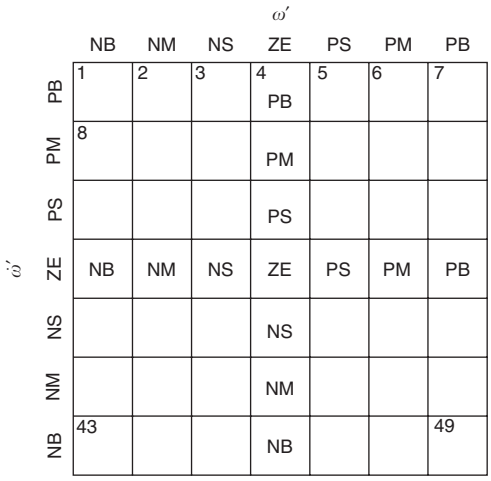

Fig. 3 *Initial fuzzy rule matrix of proposed controller*

3.2 Topology of neural fuzzy controller

The topology of the proposed NFC, as shown in Fig. 4, is a five-layer neural network-based fuzzy controller. Since two input variables and one output variable are employed in the present work, there are two nodes in layer 1 and one node in layer 5. The nodes in layers 2 and 4 are term nodes that act as membership functions to express the input/output fuzzy linguistic variables. A bell-shaped function is adopted to represent the membership functions, in which the mean value and the variance will be adapted through the learning process. The fuzzy set defined for input/output variables is positive big (PB), positive medium (PM), positive small (PS), zero (ZE), negative medium (NM) and negative big (NB), which are numbered in descending order in the term nodes. Hence, 14 nodes and 7 nodes are included in layers 2 and 4, respectively, to indicate the input/output linguistic variables. Nodes in layer 3 represent the fuzzy control rule, and there are 49 nodes in layer 3 to form a fuzzy rule base for two linguistic input variables. The links of layers 3 and 4 define the preconditions and the consequences of the rule

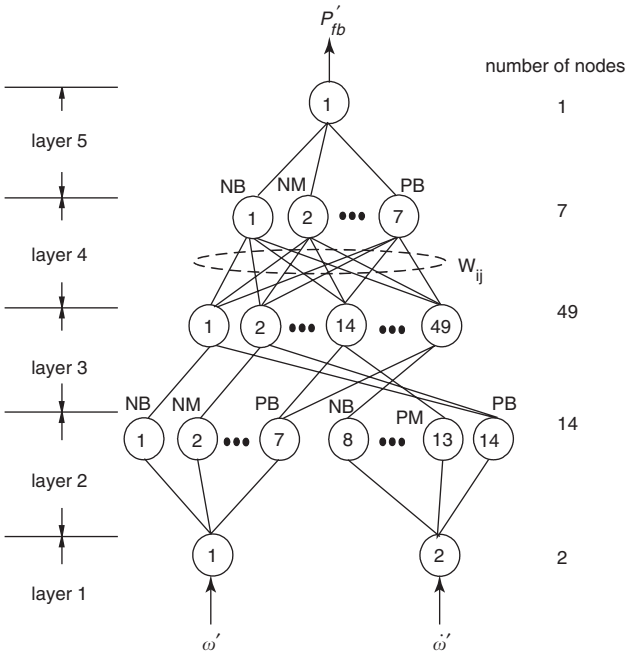

Fig. 4 *Topology of proposed NFC*

nodes, respectively. There are two fixed links from the input term nodes for each rule node. Layer 4 links encircled by the broken line are adjusted in response to varying control situations. The links of layers 2 and 5 remain fixed between the input/output nodes and their corresponding term nodes. In short, the proposed controller can adjust the fuzzy control rules and their membership functions by modifying layer 4 links and the parameters of the membership functions for each node in layers 2 and 4. As a convenience in notation, the following symbols are used to describe the functions of the nodes in each of the five layers:

NET_i^{Lj} net input value of the ith node in layer j

O_i^{Lj} output value of the ith nodes in layer j

m_i^{Lj}, σ_i^{Lj} mean and variance of bell-shaped activation function of ith mode in layer j

W_{ij} link that connects the output of the jth node in layer 3 the input to ith node in layer 4.

The schematic structure of each layer of NFC is as follows:

Layer 1: The nodes of this layer directly transmit input signals to the next layer, that is

$$O_1^{L1} = \omega' \tag{13}$$

$$O_2^{L1} = \dot{\omega}' \tag{14}$$

Layer 2: The nodes of this layer act as membership functions to express the terms of input linguistic variables. For a bell-shaped function, they are:

$$NET_i^{L2} = \begin{cases} O_1^{L1}, & \text{for } i = 1, 2, \ldots, 7 \\ O_2^{L1}, & \text{for } i = 8, 9, \ldots, 14 \end{cases} \tag{15}$$

$$O_i^{L2} = e^{-\left[\frac{NET_i^{L2} - m_i^{L2}}{\sigma_i^{L2}}\right]^2}, \quad \text{for } i = 1, 2, \ldots, 14 \tag{16}$$

The link weights in this layer are set to unity.

Layer 3: The links in this layer are used to perform preconditioned matching of fuzzy rules. Each node has two input values from layer 2. If the correlation-minimum inference procedure is used here to determine the firing strengths of each rule, then the output of nodes in the layer is determined by the fuzzy AND operation. Thus, the functions of the layer are:

$$NET_i^{L3} = min\,(O_j^{L2}, O_k^{L2}), \quad i = 7(j-1) + (k-7) \tag{17}$$

$$O_i^{L3} = NET_i^{L3}, \quad i = 1, 2, \ldots, 49; \quad j = 1, 2, \ldots 7; \quad k = 8, 9, \ldots, 14 \tag{18}$$

The link weights in this layer are also set to unity.

Layer 4: Each node in this layer performs the fuzzy OR operation to integrate the fired rules leading to the same output linguistic variable. Based on engineering knowledge concerning the dynamic nature of the generator, 13 heuristic fuzzy rules are designed in Fig. 3. The initial link weights can be set according to the initial fuzzy rules. For example, the weight of rule 4 that connects rule node 4 to the output term node 'PB' is set at unity. Except for the weights predetermined from the initial rules, the rest of layer 4 links are all set to zero initially. Based on the simulation result, starting with the good initial fuzzy control rules provides much faster convergence in the learning phase. The functions of this layer are expressed as follows:

$$NET_i^{L4} = \sum_{j=1}^{49} W_{ij} O_j^{L3} \tag{19}$$

$$O_i^{L4} = min\,(1, NET_i^{L4}), \quad \text{for } i = 1, 2, \ldots, 7. \tag{20}$$

The link weight W_{ij} in this layer indicates the probability of the jth rule with the ith output linguistic.

Layer 5: The output node in this layer together with layer 5 links act as a defuzzifier of the NFC. The defuzzification aims at producing a nonfuzzy control action that best represents the possibility distribution of an inferred fuzzy control action. The centre of area defuzzification scheme can be simulated by:

$$NET_1^{L5} = \sum_{j=1}^{7} m_j^{L4} \sigma_j^{L4} O_j^{L4} \tag{21}$$

$$O_1^{L5} = P'_{fb} = \frac{NET_i^{L5}}{\sum_{j=1}^{7} \sigma_j^{L4} O_j^{L4}} \tag{22}$$

where m and σ can be viewed as the centre and the width of the membership function. Hence the link weight in this layer is $m_j^{L4} \sigma_j^{L4}$.

3.3 Learning algorithm of proposed controller

There are learning and operation phases to implement the proposed control system. Based on simple engineering knowledge concerning the controlled machine, we set up the controller with a set of coarse fuzzy control rules. Then, the parameters of the NFC are tuned to achieve good control performance. For this purpose, a performance index table (PIT) and its related lookup table, as shown in Fig. 5, were developed. The performance of the controller in each learning step is evaluated by the PIT, from which a credit is assigned according to the deviation of the control response from the desired response. It should be noted that the PIT is developed based on the control objective. The zero elements in the lookup table are in the desired response regions, and the other regions indicate where corrective control needs to be taken. The membership functions and fuzzy rules of the NFC could be adapted online by the credit value using a

acceleration \ speed	−3.0	−2.0	−1.0	0	1.0	2.0	3.0
0.6	0	0.3	0.3	0.6	0.6	1.0	1.0
0.4	−0.3	0	0.3	0.3	0.6	1.0	1.0
0.2	−0.3	−0.3	0	0.3	0.3	0.6	0.6
0	−0.6	−0.3	−0.3	0	0.3	0.3	0.6
−0.2	−0.6	−0.6	−0.3	−0.3	0	0.3	0.3
−0.4	−1.0	−1.0	−0.6	−0.3	−0.3	0	0.3
−0.6	−1.0	−1.0	−0.6	−0.6	−0.3	−0.3	0

Fig. 5 *Lookup table of performance index*

supervised learning mechanism. For the kth learning step, the required change $\Delta P'_{fb}(k)$ of the NFC can be defined as

$$\Delta P'_{fb}(k) = \lambda \times PI[\omega'(k), \dot{\omega}'(k)] \tag{23}$$

where $PI[\cdot]$ represents lookup values in the PIT, and λ is a learning constant, which is set at 0.005 in this study. Hence the desired control action $P'^{d}_{fb}(k)$ of the NFC can be obtained by

$$P'^{d}_{fb}(k) = P'_{fb}(k) + \Delta P'_{fb}(k) \tag{24}$$

The optimal parameters of membership functions and fuzzy rules can be found by gradient-descent search techniques. The error or energy function of the control system can be defined by

$$E = \frac{1}{2}\left(P'^{d}_{fb}(k) - P'_{fb}(k)\right)^2 \tag{25}$$

From (24) and (25), the minimisation of the error function E results in guiding the controlled plant into the desired response regions where the error function reaches a local minimum. Then, the generalised delta-learning rule can be used to solve the training task of the NFC to achieve energy minimisation. In standard notation, the generalised delta-learning rule can be expressed as

$$y_i(k+1) = y_i(k) + \eta\left(-\frac{\partial E}{\partial X_i}\right) + \alpha \Delta y_i(k) \tag{26}$$

where y_i is the parameter to be updated, and η and α are the learning rate and the gain of the momentum term, which are set to 0.1 and 0.9, respectively. The error signal term δ_i^{Li} produced by the ith neuron in layer j is defined as

$$\delta_i^{Li}(k) = -\frac{\partial E}{\partial NET_i^{Lj}} \tag{27}$$

Using (26) and (27), the learning rules of each layer are derived below:

Layer 5: The error signal of the output node is

$$\delta_1^{L5} = \left(P'^{d}_{fb}(k) - P'_{fb}(k)\right) \tag{28}$$

Layer 4:

1 The error signal of each node is

$$\delta_i^{L4} = \delta_1^{L5} \frac{m_i^{L4}\sigma_i^{L4}\left(\sum_{j=1}^{7}\sigma_j^{L4}O_j^{L4}\right) - \sigma_i^{L4}\left(\sum_{j=1}^{7} m_j^{L4}\sigma_j^{L4}O_j^{L4}\right)}{\left(\sum_{j=1}^{7}\sigma_j^{L4}O_j^{L4}\right)^2}$$
$$\text{for } i = 1, 2, \ldots, 7 \tag{29}$$

2 The mean and variance of each output membership function are adapted by

$$m_i^{L4}(k+1) = m_i^{L4}(k) + \eta\delta_1^{L5}\frac{\sigma_i^{L4}O_i^{L4}}{\sum_{j=1}^{7}\sigma_j^{L4}O_j^{L4}} + \alpha\Delta m_i^{L4}(k) \tag{30}$$

$$\sigma_i^{L4}(k+1) = \sigma_i^{L4}(k) + \eta\delta_1^{L5} \times \frac{m_i^{L4}O_i^{L4}\left(\sum_{j=1}^{7}\sigma_j^{L4}O_j^{L4}\right) - \sigma_i^{L4}\left(\sum_{j=1}^{7} m_j^{L4}\sigma_j^{L4}O_j^{L4}\right)}{\left(\sum_{j=1}^{7}\sigma_j^{L4}O_j^{L4}\right)^2} + \alpha\Delta\sigma_i^{L4}(k) \quad \text{for } i = 1, 2, \ldots, 7 \tag{31}$$

3 The weight between the ith output linguistic variable and jth rule is updated by

$$W_{ij}(k+1) = W_{ij}(k) + \eta\delta_i^{L4}O_j^{L3} + \alpha\Delta W_{ij}(k)$$
$$\text{for } i = 1, 2, \ldots, 7; \quad j = 1, 2, \ldots, 49 \tag{32}$$

Layer 3: In this layer, no parameter needs to be adjusted. Only the error signal needs to be computed and propagated backward, that is,

$$\delta_i^{L3} = \sum_{j=1}^{7} W_{ij}\delta_j^{L4} \tag{33}$$

Layer 2: The mean and variance of the input membership function can be updated by

$$m_i^{L2}(k+1) = m_i^{L2}(k) - \eta\frac{\partial E}{\partial O_i^{L2}}O_i^{L2}\frac{2(O_j^{L1} - m_i^{L2})}{(\sigma_i^{L2})^2} + \alpha\Delta m_i^{L2}(k) \tag{34}$$

$$\sigma_i^{L2}(k+1) = \sigma_i^{L2}(k) - \eta\frac{\partial E}{\partial O_i^{L2}}O_i^{L2}\frac{2(O_j^{L2} - m_i^{L2})}{(\sigma_i^{L2})^3} + \alpha\Delta\sigma_i^{L2}(k) \quad \text{for } i = 1, 2, \ldots, 7; \quad j = 1, 2 \tag{35}$$

Layer 1: This layer is to distribute the input signal only. It is not involved in the learning process.

The link connecting layers 4 and 3 can be deleted when the weight is negligibly small or equals zero after learning because this rule node has little or no relationship to the output linguistic variable. The function of layer 1 is to distribute the input signal only. It is not involved in the learning process.

4 Simulations and discussion

4.1 Test conditions

The 345 kV transmission system network of Taipower system is shown in Fig. 6. The system has four main load areas, North, Center, South and East. There will be, in total, three 345 kV double-circuit corridors from south to north in Taipower in 2002. The peak demand on the Taipower system reached 26 296 MW in 2001 and the annual growth rate of peak demand is 1.7%. This system consists of six nuclear units, 57 thermal units and 19 hydro units, including ten pumped-storage units. There are two nuclear plants in the north and one nuclear plant in the south; the thrid nuclear plant is the biggest nuclear plant in Taiwan. To test the proposed methodology, the main disturbance is a three-phase short-circuit fault with various clearing times in the generator bus of the second nuclear plant. Unless otherwise stated, the FESS is installed only on generator 2 of the second nuclear plant with the others uncontrolled in the test cases. The lower limit and upper limit of the FESS power are set between −0.5 p.u. and 0.5 p.u., respectively. To evaluate the performance of the proposed controller a quadratic performance index J is defined as:

$$J = \sum_{k=1}^{200}\omega_i^2(k) \tag{36}$$

In (36), the sampling time of system measurements is set at 0.01 s, thus there are a total 200 training patterns in each learning process.

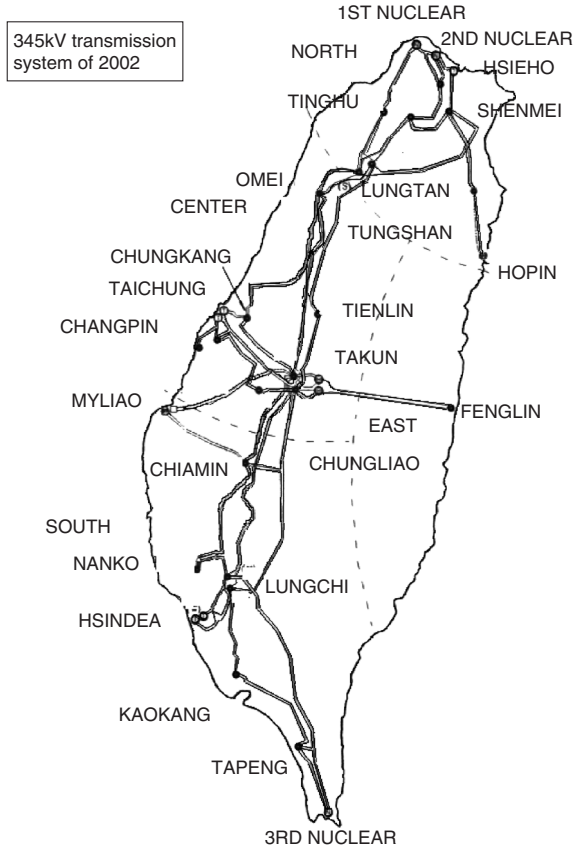

Fig. 6 *Taipower 345 kV transmission system network [1]*

4.2 Test results

To show the learning capability of the proposed controller, consider a particular three-phase fault at generator 2 of second nuclear plant with the fault cleared at 0.28 s. Figure 7 shows the curve of the performance index with respect to the number of learning epochs. It indicates that only 35 epochs are required to reach convergence. The fast learning time is due to the fact that the prior knowledge of the controller is incorporated into the training process. Figures 8 and 9 show the dynamic responses of the controlled generator between 1 and 40 epochs of learning. The results obtained apparently show that the control performance can be significantly improved through the learning process.

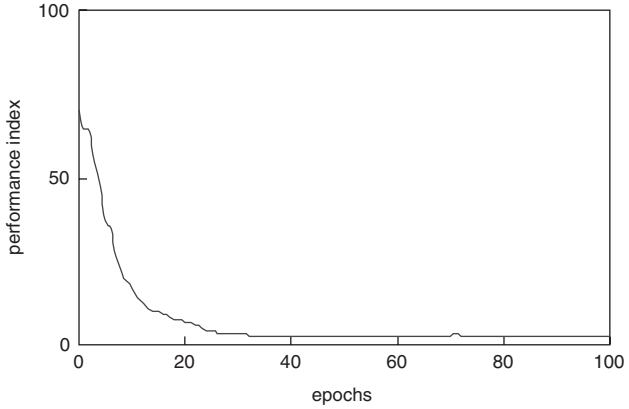

Fig. 7 *Learning curve of proposed controller*

Figure 10 shows the absorbed power and energy of FESS, the maximum power of the FESS is set in about 458 MW (or 0.5 p.u.). It is clear that the transient energy of

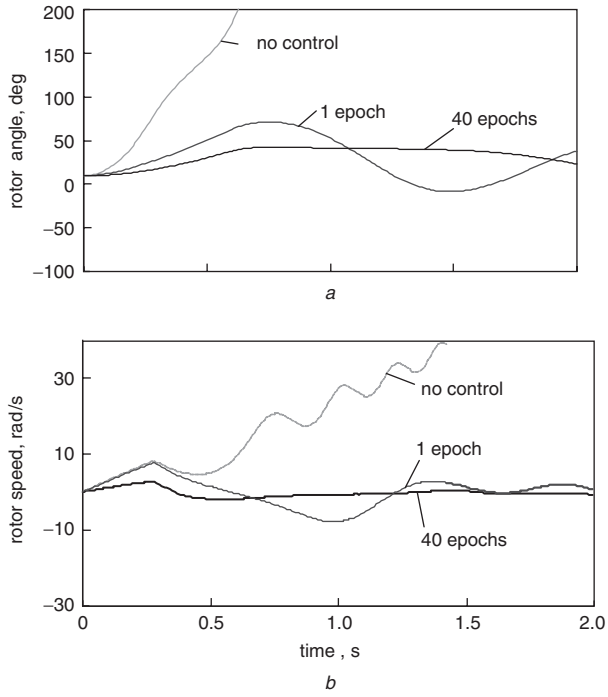

Fig. 8 *Dynamic responses of generator 2 in the second nuclear plant*
a Rotor angle
b Rotor speed

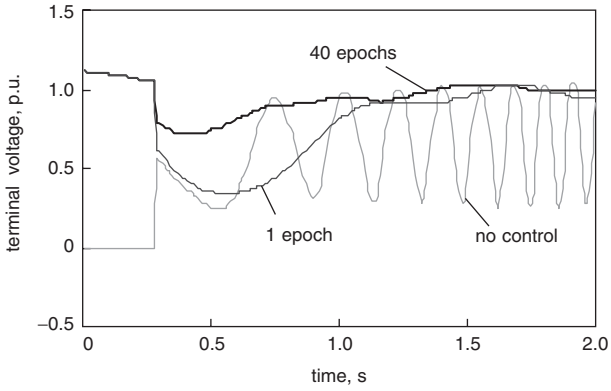

Fig. 9 *Terminal voltage responses of generator 2 in the second nuclear plant*

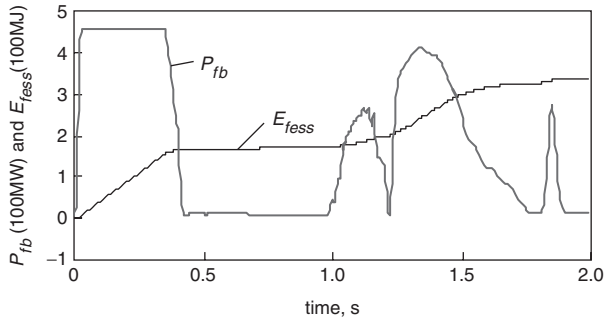

Fig. 10 *Absorbed power and energy of FESS*

the power system has been stored in the FESS, and it will be most useful for power flow control when the power system recovers its stability. Figures 11 and 12 show the membership functions of the input and output linguistic variables, before and after the learning process. Obviously, some of

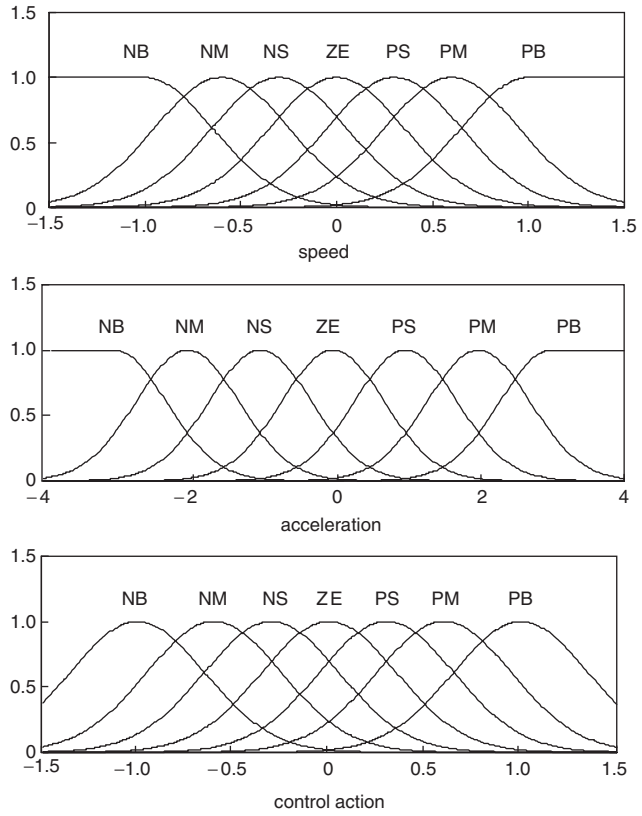

Fig. 11 *Initial membership function of proposed controller*

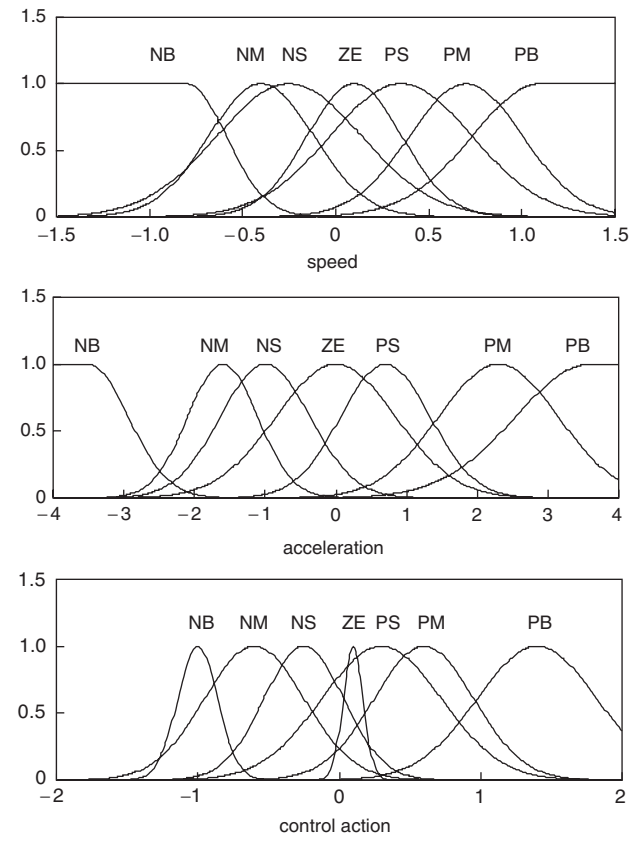

Fig. 12 *Learned membership functions of proposed controller*

the membership functions have been largely modified in appearance.

To test the effect of the proposed controller with FESS, the critical clearing time (CCT) with different capability of

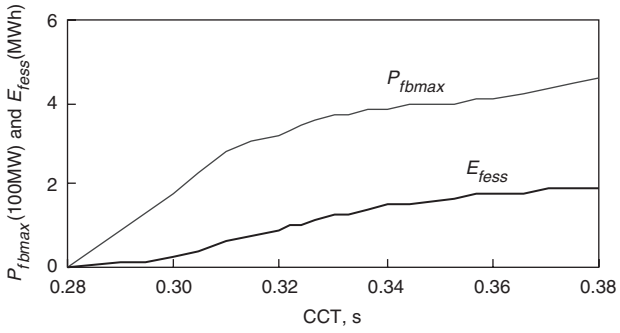

Fig. 13 *Capability of FESS with different CCT*

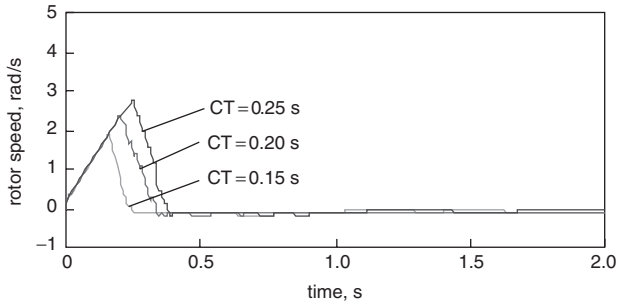

Fig. 14 *Dynamic responses of generator 2 with different fault clearing times*

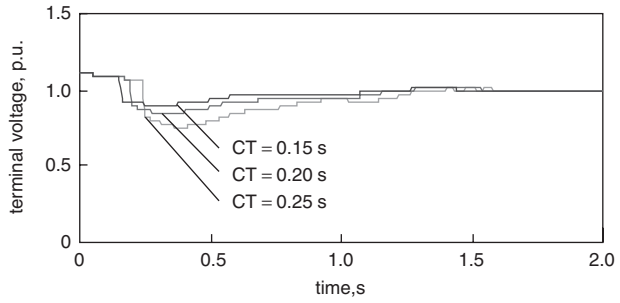

Fig. 15 *Terminal voltage responses of controlled generator with different fault clearing times*

FESS is shown in Fig. 13. The test results show that the FESS capability is the most effective method for the improvement of transient stability. It could be used to enhance the CCT of the Taiwan power system.

To test the robustness of the trained controller, consider a three-phase fault with different cleared times at generator bus 2. The dynamic responses of generator 2 with fault, cleared at 0.15, 0.2 and 0.25 s are shown in Figs. 14 and 15. Note that, although the proposed controller was trained from past control trends, it is still capable of yielding satisfactory transient responses for different disturbances. The rotor speed and terminal voltage of the controlled generator will always return to stability.

5 Conclusions

The first application of FESS in the transient stability control of power systems is presented. The FESS has been shown as one of the most useful devices for transient stability control of power systems, because the FESS can accept and deliver large amounts of energy in a very short time. Because of the nonlinear model in this control problem, an efficient self-organising neural fuzzy controller

to enhance the transient stability of a power system has been presented. The control parameter of the proposed controller can be optimally tuned from training examples by the learning algorithm. As a result of the evolving symbiosis of these new techniques, the proposed controller has shown to be more adaptive and robust in responding to different disturbances. To illustrate the performance and usefulness of the proposed method, a series time simulation was also conducted on the Taipower system with encouraging results.

6 Acknowledgments

The authors are greatly indebted to the engineers of the Taiwan Power Company for providing the valuable field test data. We also gratefully acknowledge the financial support of the National Science Council, Taiwan, Republic of China (Project No: 92-2213-E-167015).

7 References

1 Lin, C.M., Chiang., C.H., Lin, C.M., Huang, T.C., and Jalali, S.G.: 'Feasibility studies of FACTs application in the Taiwan Power Company 345 kV Transmission System'. 22nd Symp. on Electrical Power Engineering, Taiwan, 2001, pp. 234–238
2 Hingorani, N.G.: 'High power electronics and flexible AC transmission systems', *IEEE Power Eng. Rev.*, 1998, pp. 3–4
3 Larsen, E.V., Sanchez-Gaseca, J.J., and Chow, J.H.: 'Concept for design of FACTS controller to damp power system swing', *IEEE Trans. Power Systems.*, 1995, **10**, (2), pp. 948–956
4 Chang, H.C., and Wang, M.H.: 'Neural network-based self-organizing fuzzy controller for transient stability of multimachine power systems', *IEEE Trans. Energy Convers.*, 1995, **10**, (2), pp. 339–346
5 Hebner, R., Beno, J., and Walls, A.: 'Flywheel batteries come around again', *IEEE Spectr.*, 2002, pp. 46–51
6 Borneman, H.J., and Sander, M.: 'Conceptual system design of a 5 MWh/100 MW superconducting flywheel energy storage plant for power utility applications', *IEEE Trans. Appl. Supercond.*, 1997, **7**, (2), pp. 398–401
7 Weissbach, R.S., Karady, G.G., and Farmer, R.G.: 'Dynamic voltage compensation on distribution feeders using flywheel energy storage', *IEEE Trans. Power Deliv.*, 1999, **14**, (2), pp. 165–170
8 Akagi, H., and Sato, H.: 'Control and performance of a doubly-fed induction machine intended for a flywheel energy storage system', *IEEE Trans. Power Electron.*, 2002, **17**, (1), pp. 109–116
9 Cardenas, R., Pena, R., Asher, G., and Clare, J.: 'Control strategies for enhanced power smoothing in wind energy systems using a flywheel driven by a vector-controlled induction machine', *IEEE Trans. Ind. Electron.*, 2001, **48**, (3), pp. 625–635
10 Hampton, D.E., Tindall, C.E., and Mcardle, J.M.: 'Emergency control of power system frequency using flywheel energy injection'. IEE Int. Conf. on Advances in Power System Control, Operation and Management, 1991, pp. 662–667
11 Komori, M., and Akinaga, N.: 'A prototype of flywheel energy storage system suppressed by hybrid magnetic bearings with H^{∞} controller', *IEEE Trans. Appl. Supercond.*, 2001, **11**, (1), pp. 1733–1736
12 IEEE Committee Report: 'Computer representation of excitation system', *IEEE Trans. Power Appar. Syst.*, 1968, **87**, pp. 1460-1464
13 Ross, T.J.: 'Fuzzy logic with engineering applications' (Mcgraw-Hill, Inc., 2000)